

Tesi di Dottorato in Fisica degli Acceleratori

Alessandro Curcio

Supervisors: M. Petrarca and D. Giulietti

Sapienza Universita' di Roma

Roma, Ottobre 2017

Summary

Introduction

Laser-target interaction

Betatron Radiation: transverse emittance diagnostics

X-ray production from plasma filaments in front of solid targets

Laser-plasma interaction in capillary waveguides

Laser-plasma interaction for acceleration and radiation

- ★ The Ph.D. activity of the candidate Alessandro Curcio was developed at the National Laboratories of Frascati (LNF) of the INFN and at University of Rome La sapienza.
- ★ The focus was on the interaction of lasers mainly with plasmas both from a theoretical and experimental point of view.
- ★ The goal was to show that the interaction of ultra-short and/or high-power lasers with plasmas/matter paves the way to novel schemes for the design of compact accelerators and secondary sources of electromagnetic radiation from THz to $X - \gamma$ rays.
- ★ These brilliant sources can be useful for a variety of users, as well as for designing diagnostics of beams.

List of main publications

- ★ R. Pompili, M. P. Anania, F. Bisesto, M. Botton, M. Castellano, E. Chiadroni, A. Cianchi, A. Curcio, M. Ferrario, M. Galletti, Z. Henis, M. Petrarca, E. Schleifer & A. Zigler. *Femtosecond dynamics of energetic electrons in high intensity laser-matter interactions*. *Sci. Rep.* 6, 35000; doi: 10.1038/srep35000 (2016).
- ★ R. Pompili, M. P. Anania, F. Bisesto, M. Botton, M. Castellano, E. Chiadroni, A. Cianchi, A. Curcio, M. Ferrario, M. Galletti, Z. Henis, M. Petrarca, E. Schleifer & A. Zigler. *Sub-picosecond snapshots of fast electrons from high intensity laser-matter interactions*. *Optics express* 24.26 (2016): 29512-29520.
- ★ Curcio, A. et al., *Electro-optic detection of coherent radiation induced by relativistic electron bunches in near and far field*. To be published on *Physical Review Applied*.
- ★ Curcio, A., et al. "Trace-space reconstruction of low-emittance electron beams through betatron radiation in laser-plasma accelerators." *Physical Review Accelerators and Beams* 20.1 (2017): 012801.
- ★ Curcio, A., et al. "Single-shot non-intercepting profile monitor of plasma-accelerated electron beams with nanometric resolution." *Applied Physics Letters* 111.13 (2017): 133105.
- ★ Curcio, A. et al. *Characterization of X-ray radiation from solid Sn target irradiated by femtosecond laser pulses in the presence of air plasma sparks*. *Laser and Particle Beams* (2016), 34, 533538. Cambridge University Press, 2016 0263-0346/16 doi:10.1017/S0263034616000458.
- ★ Curcio, A. et al. *Numerical and analytical models to study the laser-driven plasma perturbation in a dielectric gas-filled capillary waveguide*. *Optics Letters* 41, 18; <http://dx.doi.org/10.1364/OL.99.099999> (2016).
- ★ Curcio, A., D. Giulietti, and M. Petrarca. "Tuning of betatron radiation in laser-plasma accelerators via multimodal laser propagation through capillary waveguides." *Physics of Plasmas* 24.2 (2017): 023104.

Laser-solid target interaction

- ★ *R. Pompili, M. P. Anania, F. Bisesto, M. Botton, M. Castellano, E. Chiadroni, A. Cianchi, A. Curcio, M. Ferrario, M. Galletti, Z. Henis, M. Petrarca, E. Schleifer & A. Zigler. Femtosecond dynamics of energetic electrons in high intensity laser-matter interactions. Sci. Rep. 6, 35000; doi: 10.1038/srep35000 (2016).*
- ★ *R. Pompili, M. P. Anania, F. Bisesto, M. Botton, M. Castellano, E. Chiadroni, A. Cianchi, A. Curcio, M. Ferrario, M. Galletti, Z. Henis, M. Petrarca, E. Schleifer & A. Zigler. Sub-picosecond snapshots of fast electrons from high intensity laser-matter interactions. Optics express 24.26 (2016): 29512-29520.*
- ★ *Curcio, A. et al., Electro-optic detection of coherent radiation induced by relativistic electron bunches in near and far field. To be published on Physical Review Applied.*

Electron acceleration by laser-solid target interaction/1

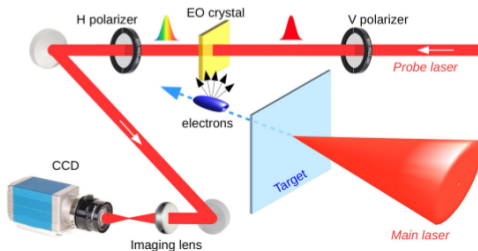


Figure: Sketch of the experiment. An $f/10$ parabola focuses the main laser on a metallic target ejecting a cloud of energetic electrons. An electro-optic crystal (ZnTe) is located 1 mm downstream the target. The Coulomb fields of the moving electrons optically modify the crystal, making it birefringent. This changing is temporally encoded by a linearly polarized probe laser. By measuring the polarization modulation of the probe laser, the main properties of the emitted electrons (charge, energy, temporal profile) are retrieved.

Electron acceleration by laser-solid target interaction/2

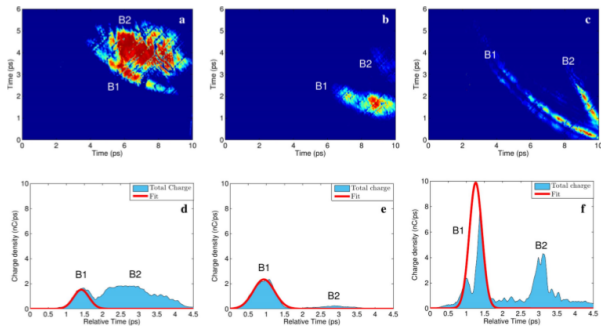


Figure: Snapshots with different target shapes. Signatures of the escaping electrons from (a) planar, (b) wedged and (c) tipped targets. The emitted charges are, respectively, (a) 1.2 nC (B1) and 3 nC (B2); (b) 2 nC (B1) and 0.3 nC (B2); (c) 7 nC (B1) and 3 nC (B2). The gaussian envelopes represent the extrapolated charge profiles of each bunch. (df) Corresponding longitudinal profiles. A 10^2 neutral density filter has been used in (b,c) to avoid saturation of the CCD camera.

Near and Far field Detection of Cherenkov Radiation/1

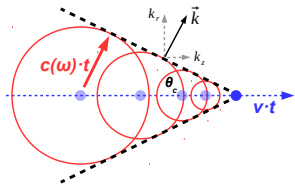


Figure: Sketch for the Cherenkov radiation formation. The charged particle (blue circle) moves from left to right with velocity $v > c(\omega) = c/n(\omega)$. The overall wave-front moves along the \vec{k} direction and is confined within a cone of aperture θ_c .

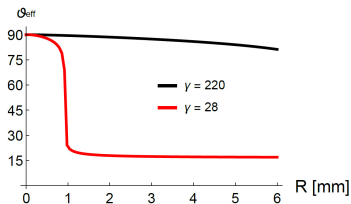


Figure: The Cherenkov angle versus the observation distance between the electrons and the crystal.

Near and Far field Detection of Cherenkov Radiation/2

8

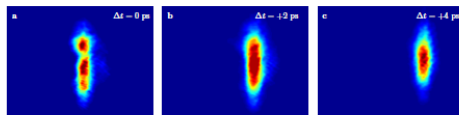


Figure 7. Experimentally measured EOS signals obtained by changing the probe laser delay (Δt) with respect to the time of arrival of the electron bunch.

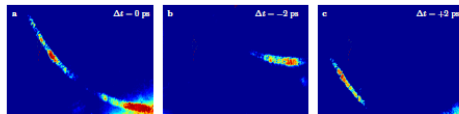


Figure 8. Experimentally measured EOS signals obtained by changing the probe laser delay (Δt) with respect to the main laser. The lack of uniformity in the experimental signals is mainly due to inhomogeneities both on the ZnTe crystal surface and on the transverse profile of the probe laser.

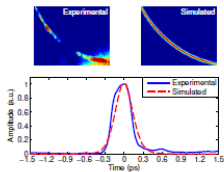


Figure 9. (Top) Experimental and simulated electro-optic signal coming electron bunches produced from the interaction of the FLAME laser with solid targets. The bunch temporal profile (bottom) is proportional to the width of the detected signal. The bunch parameters are the ones reported in Tab. I.

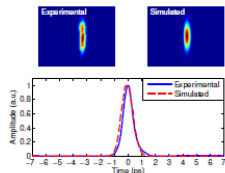


Figure 10. (Top) Experimental and simulated electro-optic signal coming electron bunches accelerated by the SPARC laser. By projecting the raw EOS signals along the horizontal axis, the bunch temporal profile (bottom) is retrieved. The bunch parameters are the ones reported in Tab. I.

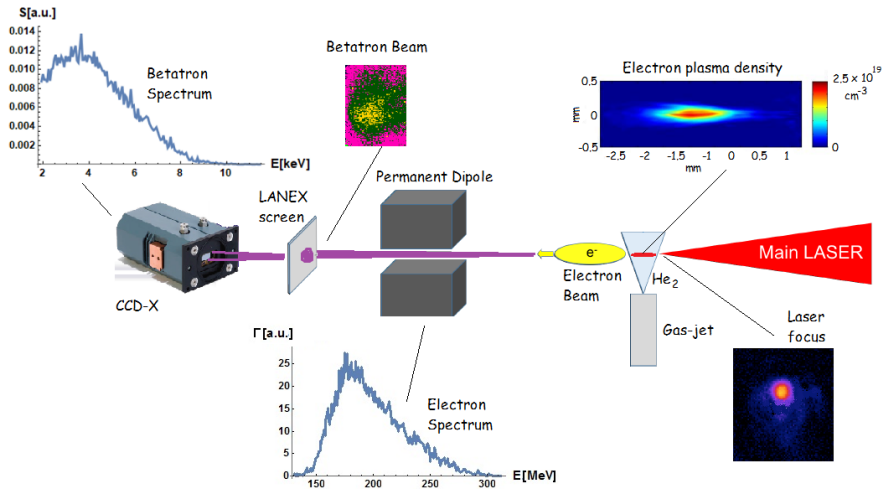
Betatron Radiation: transverse emittance diagnostics

- ★ *Curcio, A., et al. "Trace-space reconstruction of low-emittance electron beams through betatron radiation in laser-plasma accelerators." Physical Review Accelerators and Beams 20.1 (2017): 012801.*
- ★ *Curcio, A., et al. "Single-shot non-intercepting profile monitor of plasma-accelerated electron beams with nanometric resolution." Applied Physics Letters 111.13 (2017): 133105.*

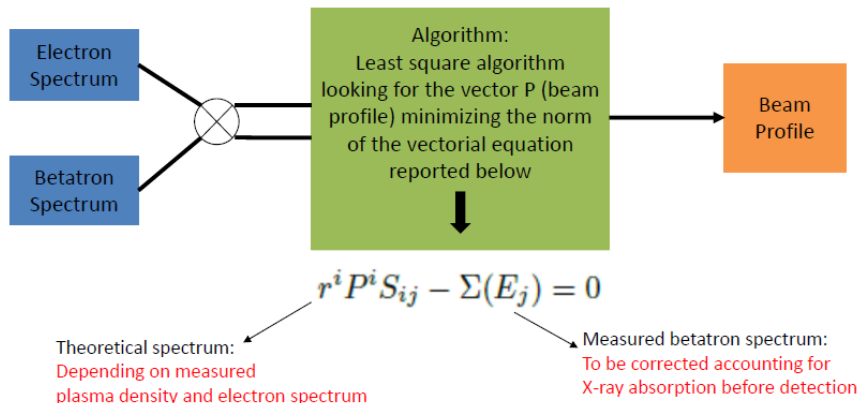
Motivations and Goals

- **Design/conceivment of a non-intercepting diagnostics for plasma accelerated electron beams**
- **Infer information about the electrons when they are still inside the plasma accelerating structure**
- **Measurement of the rms emittance, comprising the correlation term**

LWFA setup at FLAME

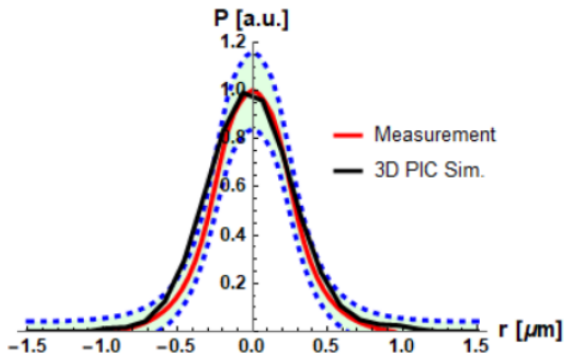


First step: beam profile retrieval/1



For details on the matrix S, see Ref. Curcio, A., et al. "Trace-space reconstruction of low-emittance electron beams through betatron radiation in laser-plasma accelerators." *Physical Review Accelerators and Beams* 20.1 (2017): 012801.

First step: beam profile retrieval/2

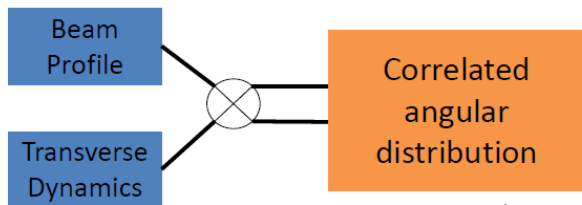


Electron beam radial profile detected (red curve) and simulated (black curve). The blue dashed curves delimit the error region (light green-shadowed).

Beam rms size $0.25 \pm 0.04 \mu\text{m}$

For discussions on the profile monitor resolution, see Ref. Curcio, A., et al. "Single-shot non-intercepting profile monitor of plasma-accelerated electron beams with nanometric resolution." To be published on *Applied Physics Letters* (2017).

Second step: angular distribution retrieval/1



$$\theta_d = \sqrt{\frac{\sqrt{1 + \frac{1}{2}\gamma_0^2 r_\beta^2 k_{\beta 0}^2}}{4\gamma_0}} r_\beta k_p$$

Correlation function
between the angle and the
position of a single electron
of the beam in the bubble

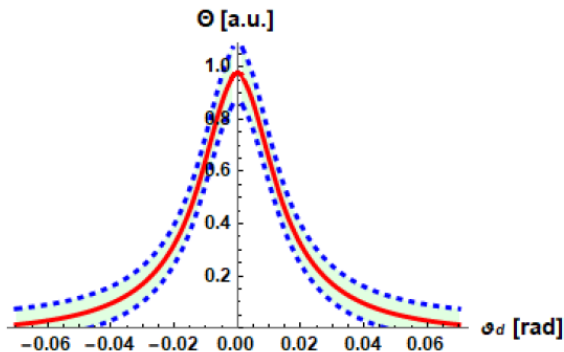
$$r_\beta = \sqrt{2}r$$

Relation between the betatron radius
and the average electron radial position
along the acceleration path

$$\Theta(\theta_d) \propto P[r(\theta_d)]$$

The angular distribution inside
the bubble is retrieved starting from
the retrieved beam profile !

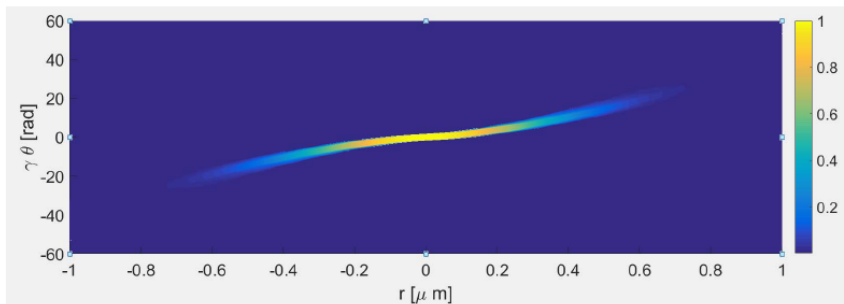
Second step: angular distribution retrieval/2



Angular distribution of the electron beam detected inside the bubble (red curve).
The blue dashed curves delimit the error region (light green-shadowed).

Beam rms divergence 13 ± 2 mrad.

Final step: Phase space reconstruction



$$\epsilon_{r\beta N} = \gamma_0 \sqrt{(\sigma_\gamma / \gamma_0)^2 \sigma_r^2 \sigma_\theta^2 + \epsilon_{r\beta}^2}$$

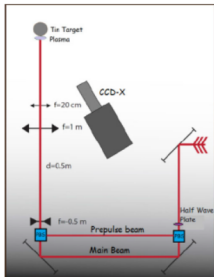
Normalized rms emittance (correlated): **0.6 mm mrad**

Normalized rms emittance (non correlated, upper limit): **1.6 mm mrad**

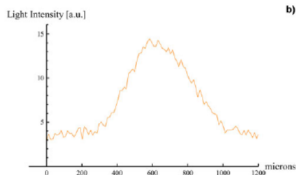
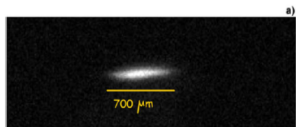
X-ray production from plasma filaments in front of solid targets

★ *Curcio, A. et al. Characterization of X-ray radiation from solid Sn target irradiated by femtosecond laser pulses in the presence of air plasma sparks. Laser and Particle Beams (2016), 34, 533538. Cambridge University Press, 2016 0263-0346/16 doi:10.1017/S0263034616000458.*

Interaction of few TW laser with air-plasma filaments/1

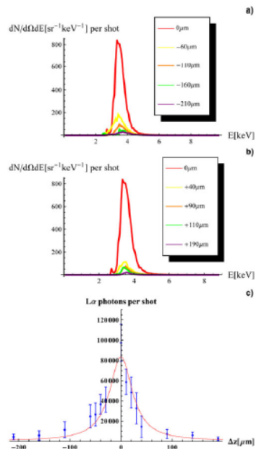


Experimental setup: the laser beam starts from the right, and then it passes through a half-wave plate in order to distribute the laser energy into the s and p polarizations in a controlled way. After this, the laser is split in polarization by a polarizing beam splitter. The delay line between the main pulse and the prepulse is 0.5 ns. A telescope is mounted with the goal to increase the beam diameter at the entrance of the last focusing lens. The two pulses are focused in air by a 20 cm positive lens. The air plasma is formed in front of the Sn target. When target is moved along the spark X-rays are observed and detected by a CCD-X in single-photon counting mode.

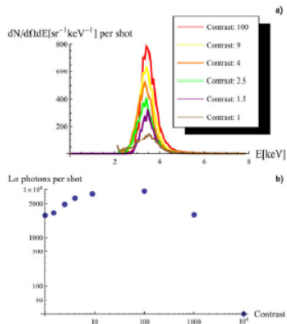


(a) Spectral and temporal integrated plasma light: longitudinal profile of the plasma spark.
(b) Line-out of the longitudinal profile of the plasma spark.

Interaction of few TW laser with air-plasma filaments/2



X-ray spectra for different negative (a, toward the incoming laser)/positive (b, in the same vs. of the incoming laser) positions of the Sn target inside the plasma channel with respect to the optimum point taken as the origin of the displacements. (c) Summary of the focus-scan results. FWHM width of the Lorentzian fit $\Delta z = 54 \mu m$.



(a) X-ray spectra for different contrast value. The target is positioned in the optimum point for the yield L_{α} photons, and then with the help of the half-wave plate the energy ratio between the main pulse and the prepulse is adjusted. (b) Number of L_{α} photons versus laser contrast. The target is positioned in the optimum point for the yield L_{α} photons.

Self-phase modulation as diagnostics

Laser phase

$$\phi = k_0 \int_0^z \mu(z, t) dz - \omega t$$

$$\omega = -\frac{d\phi}{dt}$$

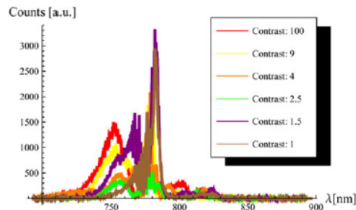
$$\omega - \omega_0 = -k_0 \int_0^z \mu(z, t) dz$$

$$\frac{d\mu}{dt} > 0 \rightarrow \text{red shift}$$

$$\frac{d\mu}{dt} < 0 \rightarrow \text{blue shift}$$

Index of refraction

$$\mu = \sqrt{1 - \frac{\omega_p^2}{\gamma \omega^2}}$$



Near-infrared laser spectra at the exit of the plasma channel for different contrast values.

Laser-plasma interaction in capillary waveguides

- ★ *Curcio, A. et al. Numerical and analytical models to study the laser-driven plasma perturbation in a dielectric gas-filled capillary waveguide. Optics Letters 41, 18; <http://dx.doi.org/10.1364/OL.99.099999> (2016).*
- ★ *Curcio, A., D. Giulietti, and M. Petrarca. "Tuning of betatron radiation in laser-plasma accelerators via multimodal laser propagation through capillary waveguides." Physics of Plasmas 24.2 (2017): 023104.*

Plasma channels in capillary waveguides/1

Propagation model:

$$\star \left[\frac{\partial^2}{c^2 \partial t^2} - \frac{2}{c} \frac{\partial^2}{\partial \zeta \partial t} \right] c_n(\zeta, t) + \frac{1}{a_{n0}^2} \sum_m P_{nm}(\zeta, t) c_m(\zeta, t) = 0$$

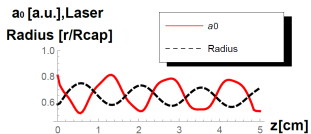
Plasma operator:

$$\star \frac{P_{nm}}{k_{p0}^2} = \langle a_n | \frac{1}{\gamma} + \frac{c^2}{2\gamma\omega_{p0}} \int_0^t dt' \sin[\omega_{p0}(t-t')] \nabla^2 (\sum_n c_n a_n)^2 | a_m \rangle$$

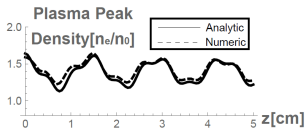
Scalar product:

$$\star \langle a_n | \hat{P} | a_m \rangle \sim 2a_{n0} a_{m0} \frac{\int_0^1 dx J_0(u_n x) \times \hat{P} J_0(u_m x)}{J_1^2(u_m)}$$

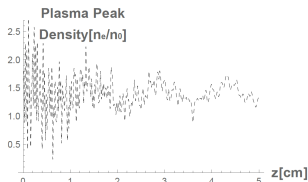
Plasma channels in capillary waveguides/2



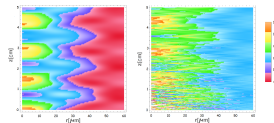
The normalized vector potential along the capillary axis and the laser beam radius normalized to the capillary radius.



The comparison between the numerical model (dashed line) and the analytical model (continuous line).



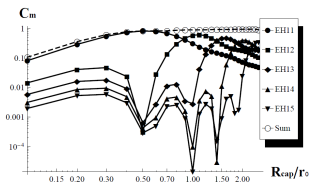
Electron plasma wave peak density along the capillary when the ionization is implemented by the ultra-short laser pulse itself.



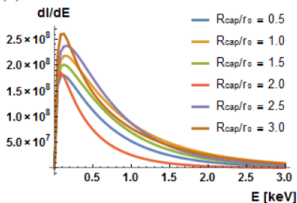
Laser intensity [a.u.] 2D map of a capillary guided pulse propagating through a preionized/non preionized (left/right) gas.

Tuning of betatron radiation with multimode propagation in waveguides

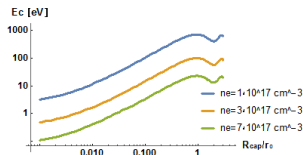
Laser mode matching



The coupling efficiency coefficients for a flat top profile laser focused into a dielectric capillary tube.



Spectrum comparison for different initial matching configurations of the laser into the waveguide ($R_{cap}/r_0=0.5, 1, 1.5, 2, 2.5, 3$).



The tuning curves of the critical energy related to the betatron radiation spectra at different background electron plasma densities.

Thanks for your attention